Stability and Multiplicity Approach to the Design of Heat-Integrated PFR

Costin S. Bildea and Alexandre C. Dimian
Dept. of Chemical Engineering, University of Amsterdam, Amsterdam, The Netherlands

The nonlinear behavior of the heat-integrated plug-flow reactor, consisting of a feed-effluent heat exchanger (FEHE), furnace, adiabatic tubular reactor, and steam generator is studied, considering a first-order, irreversible, exothermic, adiabatic reaction. Bifurcation theory is used to analyze the relationships among design, reaction thermodynamics and kinetics, and state multiplicity and stability. Hysteresis, isola and boundary-limit varieties are computed, and the influence of the activation energy, reaction heat and FEHE efficiency on the multiplicity region is studied. The double-Hopf and double-zero bifurcation points divide parameter space in regions with different dynamic behavior. State multiplicity, isolated branches, and oscillatory behavior may occur for realistic values of model parameters. A design procedure is proposed to ensure a desired multiplicity pattern and a stable point of operation and to avoid high sensitivity. The procedure was applied to three reaction systems with different kinetic and thermodynamic characteristics.

Introduction

In the autothermal PFR, heat exchange between the effluent and the feed stream is used to preheat the feed. Apparently, for an exothermic, adiabatic reaction there is no need of an additional heat source. However, there are several reasons to include a heater (normally a furnace) and a cooler (normally a steam generator) in the system:

1. A heater (furnace) is always required for startup. It may be placed upstream or downstream of the feed-effluent heat exchanger (FEHE). It is favorable to place the FEHE before the furnace, as it will work at lower temperatures. Steam can be used to generate power and/or be exported to drive separation units. This site integration solution is more efficient than process–process heat integration, as proposed by Douglas (1988).

2. Often a purge stream is available as fuel for the furnace. Consequently, a steam generator has to remove the heat excess. Placing the steam generator before the FEHE allows heat recovery at higher temperature and is therefore preferable in view of exergetic considerations.

3. In the autothermal PFR, multiple steady states may exist. Operation in the multiplicity region may be desirable or unavoidable. The classic analysis of Van Heerden (1958) shows that the middle steady state is unstable. Some states may also lose stability due to Hopf bifurcation and the system may exhibit oscillatory behavior. In such cases, stable operation is possible only if a control system is in place. If the furnace and steam generator are included, their duties are available as manipulated variables in temperature control loops.

The inclusion of furnace and steam generator leads to the structure presented in Figure 1. This structure will be called heat-integrated PFR. It should be pointed out that other series of circumstances could easily lead to other equipment arrangements.

Typical initial design data of the heat-integrated PFR are reactor type (empty tube or packed bed); feed flow rate; reactor inlet temperature; and required conversion. Reaction kinetics and thermodynamics are also known. These data are enough for one to design the reactor. Next, the designer has to size the furnace, steam generator, and FEHE. This can be done by optimizing some steady-state related economic criteria and/or considering the plantwide energy balance.

However, the operating conditions may be different. There is always uncertainty of the kinetic parameters. Feed flow rate or concentration may deviate from the design values. Disturbances in feed temperature, furnace, and steam-generator

Correspondence concerning this article should be addressed to A. C. Dimian.
Present addresses of: A. C. Dimian, Nieuwe Achtergracht 166, 1018 WV Amsterdam, The Netherlands; C. S. Bildea, University "Politehnica" Bucharest, Dept. of Chemical Engineering, Spl. Independentei 313, 77206 Bucharest, Romania.

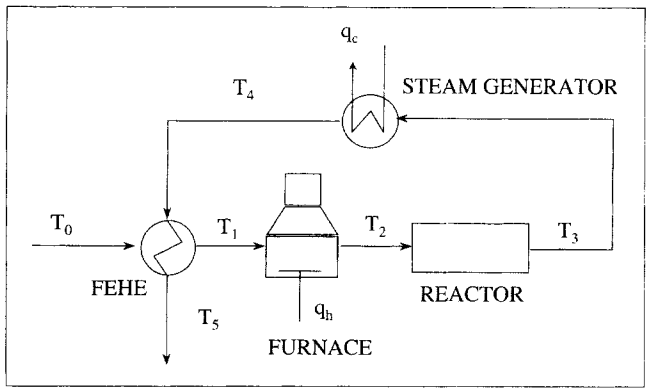

Figure 1. Heat integrated PFR.

duties are unavoidable. Heat-exchange efficiency may change due to fouling. Therefore, the operating point may become unstable and/or sustained oscillations may occur. Also, the system may exhibit high sensitivity, which renders control difficult. Consequently, the design must also be assessed with regard to steady-state multiplicity, stability, and sensitivity issues.

Many articles on the nonlinear behavior of reacting systems have been published. The first-order reaction in CSTR, axial-dispersion tubular reactor, or catalyst particle are classic problems in chemical-reaction engineering. Only a few articles, however, are dedicated to heat-integrated chemical reactors. Lovo and Balakotaiah (1992) computed the uniqueness-multiplicity boundary of the tubular reactor with internal or external heat exchange and CSTR with external heat exchange. For limiting cases, they presented analytical expressions of the ignition, extinction, and cusp points. Subramanian and Balakotaiah (1996) classified the steady state and dynamic behavior of several distributed reactor models, including the CSTR with external heat exchange and the tubular reactor with internal heat exchange.

Although singularity theory (Balakotaiah and Luss, 1982, 1984; Golubitsky and Schaeffer, 1985) and bifurcation theory (Iooss and Joseph, 1981; Scott, 1993) are proven tools, few applications to design are reported. Heiszwolf and Fortuin (1997) presented an application-oriented design procedure for unique and stable operation of first-order reaction systems in a CSTR. Morud and Skogestad (1998) discussed the dynamics of an industrial (multibed) ammonia reactor, where positive feedback due to heat integration lead to oscillatory behavior. They showed that instability occurs at a Hopf bifurcation point. Silverstein and Shinnar (1982) evaluated the stability of the heat-integrated PFR using the frequency response of individual equipment components. They did not, however, address the relationship between reaction kinetics and thermodynamics and state multiplicity and stability.

The goal of this work is to study the steady-state and dynamic behavior of the heat-integrated PFR. We consider a first-order, irreversible, exothermic reaction, and adiabatic reactor operation. We concentrate on the relationship between reaction kinetics and thermodynamics, equipment design, and state multiplicity and stability. To achieve this goal, we use elements of bifurcation theory. Moreover, we show how the results can be applied during the design, in order to ensure a desired multiplicity pattern, a stable operating point, and to avoid high sensitivity. In the next section, we present the heat-integrated PFR model equations and the types of bifurcation of interest. Afterwards, we classify the steady-state and dynamic behavior by computing the hysteresis, isola, boundary-limit, double-zero and double-Hopf varieties. State multiplicity, isolated branches, and oscillatory behavior are possible for realistic values of model parameters. We investigate the influence of reaction kinetics and thermodynamics and FEHE efficiency on the extent of multiplicity region. Subsequently, we discuss how the results can be used to avoid operational problems and propose a design procedure. Three reaction systems with different kinetic and thermodynamic characteristics are used as examples. The main ideas are reviewed in the last section. Details of the computation of the bifurcation points are given in the Appendix.

Mathematical Model

The dynamics of equipment in the heat-integrated PFR may be described by plug-flow, pseudohomogeneous models. The dimensionless equations are given below:

FEHE (tube and shell side):

$$M_t \frac{\partial \theta_t}{\partial \tau} = -\frac{\partial \theta_t}{\partial \xi} + \mathrm{NTU}\cdot(\theta_s - \theta_t)$$

$$M_s \frac{\partial \theta_s}{\partial \tau} = \frac{\partial \theta_s}{\partial \xi} - \mathrm{NTU}\cdot(\theta_s - \theta_t) \tag{1a}$$

Furnace:

$$M_h \frac{\partial \theta_h}{\partial \tau} = -\frac{\partial \theta_h}{\partial \xi} + Q_h \tag{1b}$$

Reactor:

$$\frac{\partial X}{\partial \tau} = -\frac{\partial X}{\partial \xi} + Da\cdot\exp\left(\frac{\gamma\cdot\theta_r}{1+\theta_r}\right)\cdot(1-X)$$

$$Le\frac{\partial \theta_r}{\partial \tau} = -\frac{\partial \theta_r}{\partial \xi} + B\cdot Da\cdot\exp\left(\frac{\gamma\cdot\theta_r}{1+\theta_r}\right)\cdot(1-X) \tag{1c}$$

Steam generator:

$$M_c \frac{\partial \theta_c}{\partial \tau} = -\frac{\partial \theta_c}{\partial \xi} - Q_c, \tag{1d}$$

with the boundary conditions:

$$\begin{aligned}
\theta_t(\tau,0) &= \theta_0(\tau)\\
\theta_t(\tau,1) &= \theta_h(\tau,0)\\
\theta_h(\tau,1) &= \theta_r(\tau,0)\\
\theta_r(\tau,1) &= \theta_c(\tau,0)\\
\theta_c(\tau,1) &= \theta_s(\tau,1)\\
X(\tau,0) &= 0
\end{aligned} \tag{2}$$

The model variables are dimensionless temperatures in the shell and tube side of the FEHE (θ_s, θ_t), furnace (θ_h), reactor (θ_r), steam generator (θ_c), and conversion (X). The dimensionless parameters represent reactor residence time (Da), FEHE area (NTU), activation energy (γ), adiabatic temperature rise (B), furnace and steam generator duties (Q_h, Q_c), feed temperature (θ_0), residence time ratios (M_h, M_c, M_t, M_s), and heat capacity ratio (Le).

The choice of reference temperature $\bar{T}$ deserves a special discussion. Most of the previous studies considered the Damkohler number (Da), as a bifurcation parameter, and investigated the effect of feed flow-rate change. However, feed flow rate can be easily controlled during the operation; hence, variation of this parameter is unlikely. Uncontrolled changes of feed temperature, furnace and steam generator duties, and FEHE efficiency are more probable. In the previous studies the feed temperature was chosen as reference ($\bar{T} = T_0$), becoming part of several dimensionless numbers. In this way, the dimensionless feed temperature was set to zero ($\theta_0 = 0$). When studying the steady-state behavior with feed temperature as a variable, only one dimensionless parameter must be dependent on it; hence, $\bar{T} = T_0$ is not a good choice.

If we consider isothermal operation of a fixed-size PFR, the reactant is almost completely converted ($X = 99.33\%$) for $Da = -\ln(1 - X) = 5$. We choose the corresponding reaction temperature as a reference. This is not restrictive. The reactor can be sized when the reactor inlet temperature, desired conversion, reaction kinetics, and thermodynamics are known; hence, the residence time is known. Then the reference temperature $\bar{T}$, for which $Da = 5$, can be calculated and used for dimensionless numbers. This way, changes of furnace or stream-generator duty, feed temperature and concentration, FEHE efficiency are reflected by independent changes of the model parameters: Q_h, Q_c, θ_0, B, and ϵ, respectively. Heiszwolf and Fortuin (1997) and Chen and Luss (1989) used a similar procedure setting $\gamma = 25$ and $Da = 1$, respectively.

To study the influence of flow rate on steady-state multiplicity and stability, its change must be concentrated in one parameter. This can be achieved by introducing new dimensionless variables:

$$H = \frac{K_T A_T}{\rho c_p V k(\bar{T})} \tag{3}$$

$$H_h = \frac{q_h}{\rho c_p \bar{T} V k(\bar{T})} \tag{4}$$

$$H_c = \frac{q_c}{\rho c_p \bar{T} V k(\bar{T})} \tag{5}$$

and replacing NTU, Q_h, and Q_c in Eq. 1 by $Da \cdot H$, $Da \cdot H_h$, and $Da \cdot H_c$, respectively.

The steady-state model is obtained by dropping the time derivatives in Eq. 1. After analytical integration of the FEHE, furnace, and steam-generator equations, the following boundary-value problem is obtained:

$$\frac{d\theta_r}{d\xi} = B \cdot Da \cdot \exp\left[\frac{\gamma \cdot \theta_r}{1 + \theta_r}\right] \cdot \left(1 - \frac{\theta_r - \theta_r(0)}{B}\right) \tag{6a}$$

$$f(\theta_r(0), \theta_0, Q_h, Q_c, \epsilon, B, \gamma, Da) = (1 - \epsilon)\theta_0 + (Q_h - \epsilon Q_c) + \epsilon \cdot \theta_r(1) - \theta_r(0) = 0, \tag{6b}$$

where

$$\epsilon = \frac{\text{NTU}}{1 + \text{NTU}} \tag{7}$$

is the FEHE efficiency.

The reactor conversion is given by

$$X = \frac{\theta_r(1) - \theta_r(0)}{B}. \tag{8}$$

Equation 6 may be solved by a shooting technique: start with an initial guess for $\theta_r(0)$, integrate to find $\theta_r(1)$, check the boundary condition, and update $\theta_r(0)$ (for example, by the Newton method). This way, the problem is reduced to one algebraic equation with one state variable (reactor input temperature) for which we can apply the singularity theory of a single state variable (Golubitsky and Schaeffer, 1985).

The S-shaped curves (*bifurcation diagrams*) in Figure 2 represent the conversion vs. furnace duty (*bifurcation variable*), for a given set of values of Da, γ, B, Q_c, θ_0, M_h, M_c, M_t, M_s, and Le. Each curve is associated with a fixed value of NTU. The number of possible steady states changes at *fold bifurcation points*. The upper and lower branches of the fold

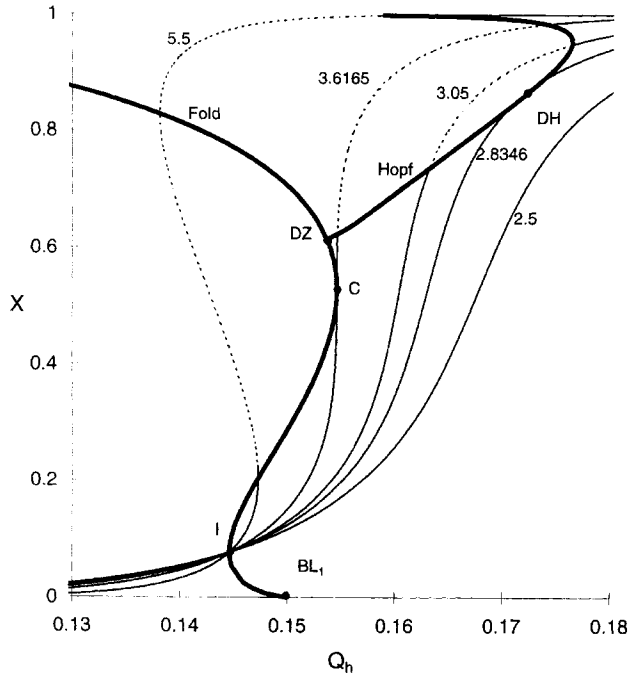

Figure 2. Conversion vs. furnace duty for different values of NTU.

$Da = 5$, $\gamma = 5$, $B = 0.07$, $\theta_0 = -0.6$, $Q_c = 0.15$, $M_t = M_s = 0.75$, $M_h = M_c = 0.2$, $Le = 2{,}000$. Continuous lines represent stable steady state. Dashed lines represent unstable steady states. Bold lines are the loci of fold and Hopf bifurcations. Points C, DH, DZ, I, and BL_1 corresponds to cusp, double-Hopf, double-zero, isola, and boundary-limit bifurcations.

curve correspond to reaction *extinction* and *ignition*, respectively. The qualitative shape of the bifurcation diagram changes when the second parameter (NTU) is varied. At the *cusp point* (C) two fold points appear or disappear and the number of steady states changes by two. The locus of cusp points is called *hysteresis variety*. Note that if the furnace duty is fixed to $Q_h \approx 0.145$ (point I), the conversion does not depend on NTU. This corresponds to an *isola* bifurcation when NTU (or ϵ) is taken as the bifurcation parameter. When the NTU parameter has very large values (NTU $\rightarrow \infty$, $\epsilon \rightarrow 1$) the bifurcation parameter on the ignition and extinction branches reaches the asymptotic values $Q_h = 0.15$ and $Q_h = 0.08$ (not shown in Figure 2), respectively. They are called *boundary-limit points* (BL). For a first-order reaction, the heat-integrated PFR exhibits at most three steady states; hence, the *double-limit* variety (where the qualitative nature of the bifurcation diagram may also change) does not exist.

When multiple steady states exist, the middle one is always unstable (dashed line). A steady state may also become unstable at a *Hopf bifurcation point*. Here a branch of oscillating solution arises. When a second parameter is varied, the number of Hopf bifurcation points may change. At the *double-Hopf* (DH) bifurcation point two Hopf bifurcation points appear or disappear. At the *double-zero* (DZ) bifurcation point, a Hopf bifurcation point appears or disappears.

Details of the bifurcation points computation are presented in the Appendix.

Steady-State Behavior

In this study we considered two cases.

First, we used as bifurcation parameter:

$$Q = (1 - \epsilon)\theta_0 + (Q_h - \epsilon Q_c). \tag{9}$$

It represents the system energy input and captures the influence of feed temperature, furnace, and steam-generator duties on the steady state. Note that θ_0, Q_h, and Q_c appear coupled as Q in the steady-state equation (Eq. 6), and they do not appear in the bifurcation equations (Eqs. A7 and A10).

A *pitchfork* bifurcation was identified. It corresponds to an isola bifurcation of the fold-points locus and divides the $\epsilon - B$ plane into two regions (Figure 3).

If the reaction is highly exothermic or the FEHE is very efficient (at the right of the pitchfork line), state multiplicity is possible irrespective of the value of the reaction activation energy. Otherwise (at the left of pitchfork line), state multiplicity is possible only for high or low activation energy.

Figure 4 presents a cross section of the hysteresis variety in $(\gamma - B)$ plane, for different values of the FEHE efficiency. For fixed ϵ, multiple steady states are possible at the right of the hysteresis line. For fixed activation energy, an increase of either the FEHE efficiency or adiabatic temperature rise leads to multiplicity. The unicity region is larger for intermediate activation energies.

Second, we considered the FEHE efficiency (ϵ) as bifurcation parameter. In this case, no other parameters may depend on it. Hence θ_0, Q_h, and Q_c may not be coupled as Q, and their effect must be investigated separately.

The steady-state behavior is more complicated. In addition to the hysteresis variety, one isola and two boundary-limit

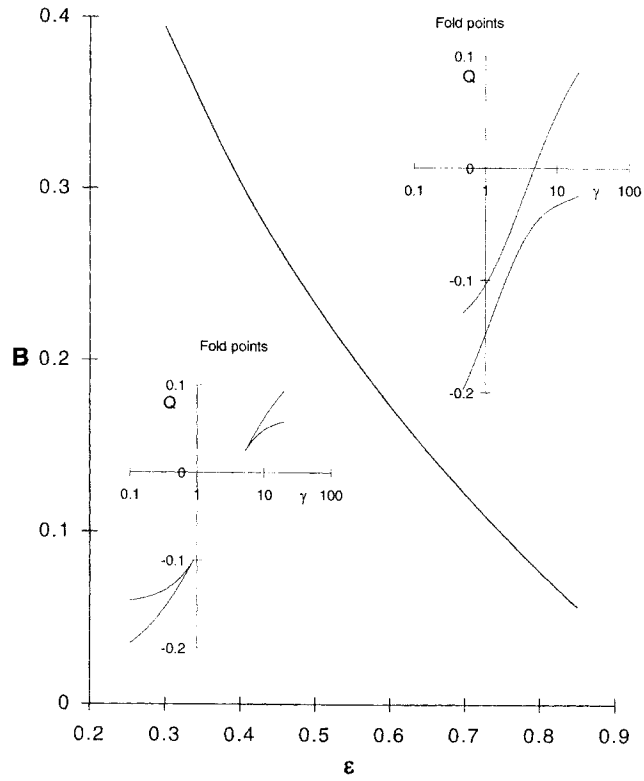

Figure 3. Pitchfork bifurcation.

At the right of pitchfork bifurcation, multiple steady states are possible irrespective of the value of activation energy.

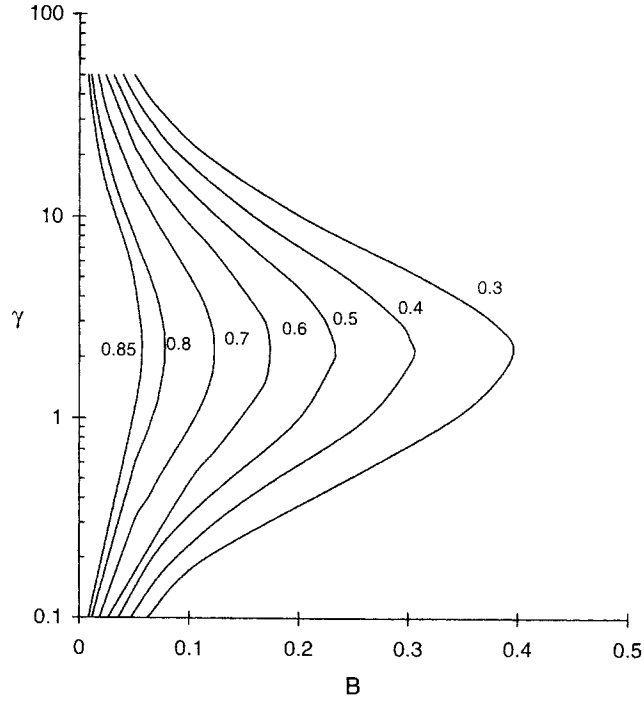

Figure 4. Cross section of the hysteresis variety in $(\gamma - B)$ plane for different values of FEHE efficiency.

For fixed ϵ, multiple steady states are possible at the right of hysteresis line.

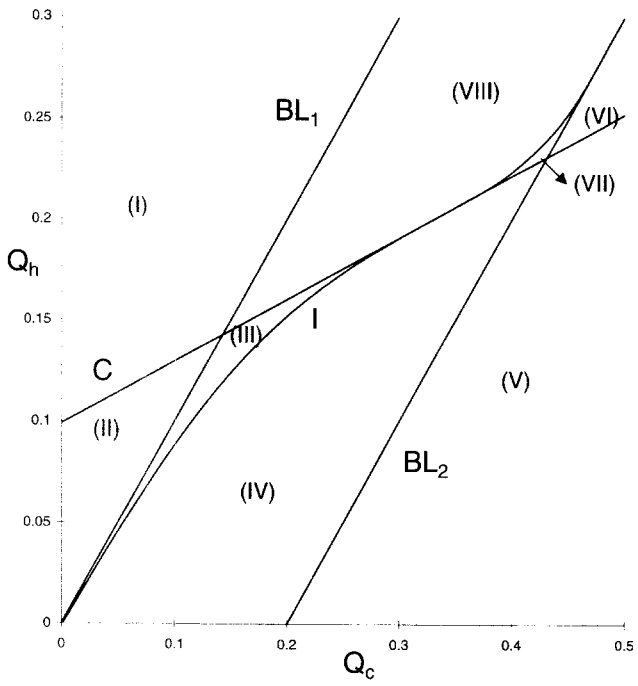

Figure 5. Phase diagram of heat-integrated PFR with FEHE efficiency as the bifurcation parameter.

$Da = 5$, $\gamma = 10$, $B = 0.2$, $\theta_0 = -0.4$. C = cusp; I = isola; BL = boundary limit. The different types of bifurcation diagrams existing in regions I–VIII are presented in Figure 6.

varieties exist. Figure 5 presents a typical phase diagram in the (Q_c, Q_h) space. The hysteresis and boundary-limit varieties are described by the following equations:

$$(1-\epsilon^*)\theta_0 + Q_h - \epsilon^* Q_c = Q^* \tag{10}$$

$$Q_h = Q_c \tag{11}$$

$$Q_h = Q_c - B, \tag{12}$$

where ϵ^* and Q^* correspond to the cusp bifurcation.

The isola variety approaches asymptotically the BL_1 and BL_2 varieties. This observation together with Eqs. 10–12 can be used to sketch the phase diagram. The isola and hysteresis varieties intersect at a pitchfork bifurcation point.

These singularities divide the parameter space into eight regions where qualitatively different bifurcation diagrams exist (they are presented in Figure 6). In region I there is a unique steady state. Crossing the hysteresis variety to region II, two fold points appear and state multiplicity is possible. When the BL_1 variety is crossed to region III, a low-conversion isolated branch appears and the multiplicity pattern becomes 1-3-1-3. The two branches coalesce when the isola is intersected and two fold points disappear. Hence, in region IV, a low conversion branch exists for all values of FEHE efficiency, while high conversion is possible only for high values of the ϵ parameters. When moving to regions V or VII, the high conversion branch disappears (at BL_2), or multiple states appear on the low-conversion branch (at hysteresis), respectively. From region VII, the high conversion branch disappears at BL_2 (region VI), or the two branches coalesce at isola (region VIII).

Note that isolated branches exist between the BL_1 and BL_2 varieties.

Dynamic Behavior

Dynamic classification involves dividing the parameter space into regions where a different number of Hopf bifurcation points exist. Due to the large number of parameters, a complete classification is difficult. We consider the energy input as the bifurcation parameter and restrict our analysis to the influence of the dimensionless adiabatic temperature rise. We focus on high values of the FEHE efficiency, and thus, high tube and shell residence times. We consider a catalytic reactor because its "wrong-way" behavior is the cause of oscillations (and hence, of Hopf bifurcations). This is reflected in the large value of *Le*.

The wrong-way behavior of packed-bed reactors has been demonstrated by Mehta et al. (1981), who used the plug-flow pseudohomogeneous model. Pinjala et al. (1988) and Chen and Luss (1989) added more complexity. They showed that models including axial dispersion and/or heterogeneity (1) account for state multiplicity inside the reactor, and (2) predict smaller and slower temperature peaks. The first matter is usually avoided in practice by the reactor design, however, and the second item does not change the qualitative transient behavior. Besides, the heat-integrated PFR becomes a *two-state-variables* problem when heterogeneity or axial dispersion is included; thus, the classification methodology is not

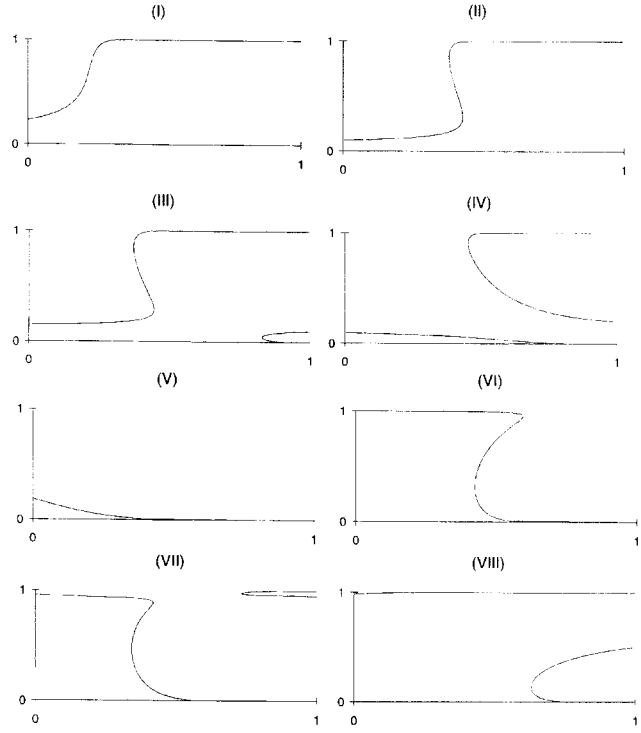

Figure 6. Conversion vs. FEHE efficiency bifurcation diagrams.

Diagrams I–VIII correspond to regions I–VIII in Figure 5.

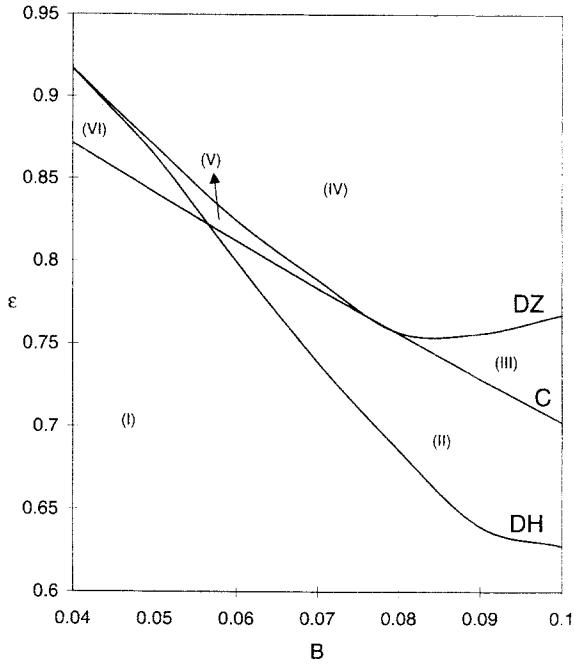

Figure 7. Phase diagram of the heat-integrated PFR with energy input as bifurcation parameter.

$Da = 5$, $\gamma = 5$, $M_t = M_s = 0.75$, $M_h = M_c = 0.2$, $Le = 2{,}000$. C = cusp; DH = double Hopf; DZ = double zero. The different types of bifurcation diagrams existing in regions I–VI are presented in Figure 8.

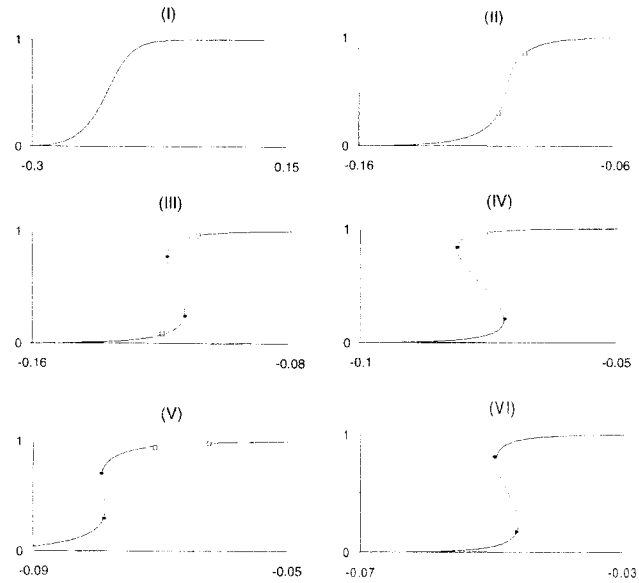

Figure 8. Conversion vs. energy input bifurcation diagrams.

Diagrams I–VI correspond to regions I–VI in Figure 7. ● = fold point; □ = Hopf point.

applicable. For these reasons, the use of the plug-flow pseudohomogeneous model is adequate for the purpose of this work. The more complex models are the subject of future research.

A typical phase diagram is presented in Figure 7. The double-zero locus is tangential to the cusp locus. The double Hopf intersects the double zero at a bifurcation point of codimension 3. The $(\epsilon - B)$ space is divided into six regions where different types of bifurcation diagrams exist. The bifurcation diagrams of conversion vs. energy input are presented in Figure 8. In region I, one stable steady state exists. After crossing the double-Hopf locus, two Hopf points appear. In between, no stable steady state exists and the system exhibits oscillatory behavior. When the hysteresis variety is crossed, two fold points appear. Therefore, in region III there are multiple steady states. Oscillatory behavior is possible on both the ignited and extinguished branches. In region IV, one Hopf point disappears after crossing the double-zero locus. In region V, a second Hopf point appears on the ignited branch. They both disappear when the double-Hopf variety is crossed; thus, in region VI steady-state multiplicity is possible but not the oscillatory behavior.

Note that the phase diagram may change (the double-zero and double-Hopf loci do not intersect) when a third parameter is varied.

It is expected that the steady-state and dynamic behavior of the heat-integrated PFR will change when a control system (for example, manipulating furnace duty to control reactor input temperature) is present. In addition, we expect more complicated phase diagrams when more detailed models are used for the furnace and steam generator (for example, with burn gas and cooling water temperatures as parameters, instead of furnace and steam-generator duties).

Design Procedure for the Heat-Integrated PFR

In this section we propose a design methodology for the heat-integrated PFR. We are not concerned with detailed sizing of the equipment. We are interested in the values of FEHE efficiency, furnace, and cooler duties. These can be obtained by optimization according to economic criteria, but certain restrictions arise when multiplicity, sensitivity, and stability are considered.

We propose the following design procedure for the heat-integrated PFR:

Step 0. Initial data: feed flow rate and concentration; reactor inlet temperature; conversion; reactor type (catalytic or empty tube); reaction kinetics and thermodynamics.

Step 1. Size the reactor based on adiabatic PFR equations.

Step 2. Choose the reference temperature. If $\overline{T}$ is chosen such that $Da = 5$, Figures 3 and 4 can be used during Step 3. Calculate the dimensionless activation energy and adiabatic temperature rise.

Step 3. Select the FEHE, based on the following observations:

- When the heat-integrated PFR is designed for low conversion, the hysteresis variety is a conservative boundary against runaway (Balakotaiah et al., 1995; Patil et al., 1997). In this case, Figure 4 can be used to select FEHE efficiency so the (γ, B) point is in the unicity region.
- When the system is designed for middle or high conversion, autothermal operation may be of interest. This is possible only when an ignited state exists. In this case, the (γ, B)

point must be in the multiplicity region of Figure 4. The extinction point gives the minimum energy input required.

- Close to the hysteresis variety the system is very sensitive to change of feed temperature, furnace, and cooler duties.
- The energy input is given by:

$$Q = (1 - \epsilon) \cdot \theta_r(0) - \epsilon \cdot B \cdot X. \tag{13}$$

Step 4. Stability issues: the middle operating point is always unstable. The other operating points may be stable or unstable. Dynamic simulation may be used to assess the stability, but no information about the extent of the stability region will be obtained. We recommend computing the Hopf bifurcation points (which are on the boundary of the oscillatory behavior region) in order to find possible instability near the operating point. Note that working at an unstable operating point is not, by itself, unattractive, as a temperature controller may stabilize the system. Loss of stability due to disturbances or design-parameter uncertainty is dangerous. If the dynamic behavior is not satisfactory, the design must be changed. The following observations should be considered:

- The whole ignited branch (high conversion) is stable (region VI in Figure 7) only for a small range of model parameters. A domain of oscillatory behavior bounded by Hopf and extinction points (regions III and IV) is very likely. In this case, increasing the energy input will stabilize the system, without significant change of conversion. If the heat of reaction is small, two Hopf points may bind the oscillation domain (region V). In this case, decreasing the energy input may also stabilize the system. This solution may be undesirable, as the operating point will move closer to the extinction point. Also, the change of the conversion will be more important.
- If the system is designed in the unicity region, oscillations are likely for highly exothermic reactions, especially at intermediate conversion (region II in Figure 5). In this case, decreasing the FEHE efficiency will ensure a stable and unique operating point.
- If no solution can be found, then some of the initial data have to be modified.

Step 5. Choose feed-temperature, furnace, and steam-generator duties. When the FEHE efficiency is constant, the bifurcation behavior depends only on the energy input (Q) and does not depend on the distribution of the energy input between feed-temperature, furnace, and steam-generator duties. Consequently, these variables can be linked to plant energy balance, site integration, combined heat and power production, or low equipment cost considerations. To prevent operational problems due to isolated branches when FEHE efficiency may change, operation in region I or II of Figure 5 should be preferred. As these regions are at the left of the BL_1 line, the following condition must be fulfilled:

$$0 < Q_c < (\theta_2 - \theta_0) - \frac{\epsilon}{1 - \epsilon} \cdot B \cdot X. \tag{14}$$

Note that the ranges for furnace and steam-generator duties decrease when the FEHE efficiency increases.

We shall illustrate the proposed methodology by three different reaction systems. The first one, propylene chlorination, is highly exothermic with moderate activation energy. Smith (1970) gives kinetic parameters. With excess propylene, the reaction can be considered first order. The second system involves a mild exothermic reaction with high activation energy: toluene hydrodealkylation (Douglas, 1988). The third system is a catalytic reaction with intermediate heat effect and low activation energy. Table 1 contains the initial data and the results.

Table 1. Design Results for Three Heat-Integrated PFR Systems*

	Propylene Chlorination	Benzene Hydrodealkylation	Catalytic Reaction
k_0	3.417×10^4	7.36×10^{10}	8.67×10^{-3}
E_a	63,070	142,870	41,430
ΔT_{ad}	170	70	70
Reaction type	Homogeneous	Homogeneous	Catalytic
T_0	300	300	300
T_2	573	910	700
X	0.995	0.75	0.53
Requirements	Autothermal operation	Autothermal operation	Unique, stable operating point
t_0	7.57	34.6	25
$\bar{T}$ (for which $Da = 5$)	700	972	1,000
γ	10.87	35	5
B	0.243	0.072	0.7
θ_0	−0.57	−0.69	−0.7
θ_2	−0.181	−0.062	−0.3
ϵ^*	0.21	0.288	0.78
Q^*	−0.192	−0.0609	−0.0947
Multiplicity	Multiple steady states if $\epsilon > 0.3$, $Q < -0.155$	Multiple steady states if $\epsilon > 0.35$, $Q < 0.058$	State unicity if $\epsilon < 0.7$, $Q > 0.116$
Stability	No oscillatory behavior is expected	Unstable operating point	Unicity does not ensure stability
FEHE efficiency	$\epsilon = 0.5$	$\epsilon = 0.6$	$\epsilon = 0.5$
No isolated branches	$Q_c < 0.147$	$Q_c < 0.547$	$Q_c < 0.344$

*The required units are given in the Notation section.

Both kinetic (k_0 and E_a) and thermodynamic data (ΔT_{ad}) are known. Design specifications are expressed as feed temperature (T_0), reactor inlet temperature (T_2), and desired conversion (X). In the first two cases, we require autothermal operation (defined by the existence of an ignited state for some range of operating variables). In the last case, we require a unique, stable operating point.

First, we design the reactor using the adiabatic PFR equations. This gives the residence time (t_0). Now we can calculate the reference temperature (for which $Da = 5$) and use it for dimensionless parameters. We mention that the dimensionless activation energy is high for the second reaction ($\gamma = 35$) and low for the third one ($\gamma = 5$). Also, the dimensionless temperature rise correctly indicates that the first reaction is highly exothermic ($B = 0.243$). Consequently, the proposed choice of the reference temperature gave meaningful results.

To get state unicity (multiplicity) we might calculate the FEHE efficiency at the cusp bifurcation (ϵ^*) and choose a lower (higher) value. Alternatively, we can simply use Figure 4 to place the (B, γ) point in the desired region.

Next, we consider stability issues. For noncatalytic reactions (first system), the high conversion branch is stable and no oscillatory behavior is expected. The second system must be operated on the middle branch, which is always unstable; hence, a stabilizing controller must be installed. For catalytic reactions (third system), unicity does not ensure stability. Figure 7 suggests that FEHE efficiency must be further decreased to ensure stable operation (region I).

After the stability was taken into account, we may choose the FEHE efficiency and use Eq. 13 to calculate the system energy input.

Finally, we must divide the energy input between feed-temperature, furnace, and steam-generator duties. Isolated branches for varying FEHE efficiency are undesirable. To avoid them, we use Eqs. 10–12 to draw diagrams similar to Figure 4, and place the operating point in region I.

Conclusions

In this article, we analyzed the relation between the reaction characteristics, design, and state multiplicity and stability of the heat-integrated PFR. We considered a first-order, irreversible, exothermic reaction.

First, the energy input was considered as the bifurcation parameter. It captures the influence of the feed-temperature, furnace, and steam-generator duties on the state multiplicity and stability. The hysteresis, double-zero, and double-Hopf bifurcation points were used to classify the steady-state and dynamic behavior of the system. The parameter space is divided into six regions, corresponding to different types of bifurcation diagrams. State multiplicity is likely for very exothermic reactions or high FEHE efficiency, irrespective of the activation energy. The heat-integrated PFR may exhibit oscillatory behavior for realistic values of model parameters.

Subramanian and Balakotaiah (1996) obtained similar phase diagrams for different adiabatic reactor models, when the Damkohler number was considered to be the bifurcation parameter. However, these systems do not exhibit oscillatory behavior for practical values of model parameters.

Second, the FEHE efficiency was chosen as the bifurcation parameter. The hysteresis, isola, and boundary limit varieties were used to classify the steady-state behavior. The parameter space is divided into eight regions where qualitative, different bifurcation diagrams exist. State multiplicity and isolated branches are now possible.

A systemic design procedure was proposed. We found that the selection of FEHE efficiency is the critical step to achieving the desired state multiplicity and ensure stability. When feed-temperature, furnace, and steam-generator duties are the changing variables, multiplicity, and stability are not affected by the partition of energy input between these variables. Consequently, the heat equipment may be designed based on plant energy balance, site integration, combined heat and power production, or lowest equipment cost. Certain restrictions arise, however, when a change of FEHE efficiency is taken into account. The procedure was applied to three reaction systems with different kinetic and thermodynamic characteristics.

The approach we presented can be applied to other equipment arrangements as well as to more complex reaction systems. Also, more accurate models of the furnace, steam generator, and catalytic reactor can be considered.

Acknowledgment

We would like to acknowledge the financial support provided for C. S. Bildea by "The Graduate School for Process Technology" (OSPT), The Netherlands.

Notation

A_f = FEHE area, m^2
c_p = specific heat, J/kg·K
E_a = activation energy, J/kmol
F = mass flow rate, kg/s
K_f = FEHE heat-transfer coefficient, $W/m^2 \cdot K$
k = reaction constant, s^{-1}
L = length, m
Le = Lewis number, dimensionless
$= 1 + \dfrac{1-\epsilon_{ff}}{\epsilon_{ff}} \dfrac{\rho_{sf} c_{p,sf}}{\rho_{ff} c_{p,ff}}$
NTU = number of transfer units, dimensionless
$= (K_f A_f)/Fc_p$
q_k = duty ($k = h, c$), J/s
Q_k = duty ($k = h, c$), dimensionless
$= q_k/(Fc_p\bar{T})$
R = gas constant, J/kmol·K
u, v = eigenfunctions
z = axial coordinate, m
V = reactor volume, m^3
ϵ = FEHE efficiency
λ = eigenvalue
ρ = density, kg/m^3
τ = time, dimensionless
$= t/t_0$
ξ = axial coordinate, dimensionless
$= z/L$

Subscripts

sf = solid phase
ff = fluid phase
b = feasibility boundary
1 = furnace inlet
3 = reactor outlet
4 = steam generator outlet

Literature Cited

Balakotaiah, V., and D. Luss, "Structure of the Steady-State Solutions of Lumped-Parameter Chemically Reacting Systems," *Chem. Eng. Sci.*, **37**, 1611 (1982).

Balakotaiah, V., and D. Luss, "Global Analysis of the Multiplicity Features of Multi-Reaction Lumped-Parameter Systems," *Chem. Eng. Sci.*, **39**, 865 (1984).

Balakotaiah, V., D. Kodra, and D. Nguyen, "Runaway Limits for Homogeneous and Catalytic Reactors," *Chem. Eng. Sci.*, **50**, 1149 (1995).

Chen, Y. C., and D. Luss, "Wrong-Way Behavior of Packed-Bed Reactors: Influence of Interphase Transport," *AIChE J.*, **35**, 1148 (1989).

Douglas, J. M., *Conceptual Design of Chemical Processes*, McGraw-Hill, New York (1988).

Golubitsky, M., and D. G. Schaeffer, *Singularities and Groups in Bifurcation Theory*, Springer-Verlag, New York (1985).

Heiszwolf, J., and J. Fortuin, "Design Procedure for Stable Operation of First-Order Reaction Systems in a CSTR," *AIChE J.*, **43**, 1060 (1997).

Iooss, G., and D. D. Joseph, *Elementary Stability and Bifurcation Theory*, Springer-Verlag, New York (1981).

Lovo, M., and V. Balakotaiah, "Multiplicity Features of Adiabatic Autothermal Reactors," *AIChE J.*, **38**, 101 (1992).

Mehta, P. S., W. N. Sams, and D. Luss, "Wrong-Way Behavior of Packed-Bed Reactors: 1. The Pseudo-Homogeneous Model," *AIChE J.*, **27**, 234 (1981).
Morud, J. C., and S. Skogestad, "Analysis of Instability in an Industrial Ammonia Reactor," *AIChE J.*, **44**, 888 (1998).
Patil, V., S. Subramanian, and V. Balakotaiah, "Singularity Theory Approach for Calculating the Runaway Boundaries of Heterogeneous Reactor Models," *Ind. Eng. Chem. Res.*, **36**, 3230 (1997).
Pinjala, V., Y. C. Chen, and D. Luss, "Wrong-Way Behavior of Packed-Bed Reactors: II. Impact of Thermal Dispersion," *AIChE J.*, **34**, 1663 (1988).
Scott, S. K., *Chemical Chaos*, Clarendon Press, Oxford (1993).
Seydel, R., "A Continuation Algorithm with Step Control," *Numerical Methods in Bifurcation Problems*, T. Kupper et al., eds., ISNM, **70**, Birkhäuser, Basel, Switzerland, p. 480 (1994).
Seydel, R., and V. Hlavacek, "Role of Continuation in Engineering Analysis," *Chem. Eng. Sci.*, **42**, 1281 (1987).
Silverstein, J., and R. Shinnar, "Effect of Design on the Stability and Control of Fixed Bed Catalytic Reactors with Heat Feedback: 1. Concepts," *Ind. Eng. Chem. Process Des. Dev.*, **21**, 241 (1982).
Smith, J. M., *Chemical Engineering Kinetics*, McGraw-Hill, New York (1970).
Subramanian, S., and V. Balakotaiah, "Classification of Steady-State and Dynamic Behavior of Distributed Reactor Models," *Chem. Eng. Sci.*, **51**, 401 (1996).
Van Heerden, C., "The Character of the Stationary State of Exothermic Processes," *Chem. Eng. Sci.*, **8**, 133 (1958).

Appendix: Bifurcation Points Computation

The equations describing the dynamic behavior of the heat-integrated PFR can be written in the following condensed form:

$$C\frac{\partial y}{\partial \tau} = -\frac{\partial y}{\partial \xi} + f(y, \mu, p) \tag{A1a}$$

$$\begin{aligned} Ay(\tau, 0) + By(\tau, 1) - c &= 0 \\ y(0, \xi) &= y_0(\xi), \end{aligned} \tag{A1b}$$

where y is the vector of model variables; C is a diagonal capacity matrix; $f(y)$ is a nonlinear function; μ is the bifurcation parameter; p is the vector of remaining parameters; A and B are constant matrices; and c is a constant vector.

Its steady-state solution is given by the boundary-value problem:

$$\frac{\partial y_s}{\partial \xi} = f(y_s, \mu, p) \tag{A2a}$$

$$Ay_s(0) + By_s(1) - c = 0. \tag{A2b}$$

When Eq. A1 is linearized around steady state, and the separation of variables is applied, the following eigenvalue problem is obtained:

$$C(\lambda_1 + \lambda_2 i)(u + iv) = -\frac{d(u + iv)}{d\xi} + f_y \cdot (u + iv) \tag{A3}$$

where

$$\delta_y = [y(\xi, \tau) - y_s(\xi)] = [u(\xi) + iv(\xi)] \cdot e^{(\lambda_1 + i\lambda_2)\tau}. \tag{A4}$$

At fold points, one real eigenvalue crosses the imaginary axis. Substitution of $\lambda_1 = \lambda_2 = 0$ in Eq. A3 and identification of real and imaginary parts gives

$$\frac{du}{d\xi} = f_y \cdot u, \tag{A5a}$$

with the boundary condition

$$Au(0) + Bu(1) = 0. \tag{A5b}$$

The eigenfunctions can be determined up to a multiplicative constant. Hence $u(0)$ may be given an arbitrary value. We have two equations for two unknowns: the state variable y and the bifurcation parameter μ. Shooting technique is available as solution method.

For the heat-integrated PFR, the FEHE, furnace, and steam-generator differential equations defining the fold points may be integrated analytically, to give

$$\begin{aligned} \frac{du_r}{d\xi} = B \cdot Da \cdot \exp\left[\frac{\gamma\theta_r}{1 + \theta_r}\right] \\ \cdot \left(\left(1 - \frac{\theta_r - \theta_r(0)}{B}\right)\frac{\gamma}{(1 + \theta_r)^2} - \frac{1}{B}\right) \cdot u_r \end{aligned} \tag{A6a}$$

$$\epsilon \cdot u_r(1) - u_r(0) = 0. \tag{A6b}$$

The fold bifurcation points of the heat-integrated PFR were found by solving the boundary-value problem defined by Eqs. 6 and A6.

The computation of the cusp points (hysteresis variety) is based on the following observation: the loci of the ignition and extinction points meet at the cusp point.

For the case of one algebraic equation (Eq. 6) with one state variable ($y = \theta_r(0)$), the defining condition for the isola variety is

$$f(y, \mu, p) = \frac{\partial f(y, \mu, p)}{\partial y} = \frac{\partial f(y, \mu, p)}{\partial \mu} = 0. \tag{A7}$$

Subramanian and Balakotaiah (1996) showed how to compute the isola variety in distributed parameter systems. However, we used a simpler approach: at the isola point, the fold locus has a local extreme. Note that all the steady solutions corresponding to varying NTU (or ϵ) pass through point I in Figure 2. Consequently, this point satisfies Eq. A7 if NTU (or ϵ) is considered as a bifurcation parameter.

If the fold point is located at a feasibility boundary, we speak about a *boundary-limit* point, defined by

$$\begin{aligned} f(y, \mu, p) = \frac{\partial f(y, \mu, p)}{\partial y} = 0 \\ y = y_b, \quad \text{or} \quad \mu = \mu_b. \end{aligned} \tag{A8}$$

State multiplicity is possible for nonzero values of the FEHE efficiency (ϵ). When this parameter approaches the limit $\epsilon = 1$, the conversion at the ignition and extinction points goes toward $X = 0$ and $X = 1$, respectively. In these cases,

the heat balance equations (Eqs. 6b and 8) reduce to Eqs. 11 and 12.

At Hopf bifurcation points, a pair of complex eigenvalues crosses the imaginary axis. Substitution of $\lambda_1 = 0$ in Eq. A3 and identification of real and imaginary parts gives

$$\begin{aligned} \frac{\partial u}{\partial \xi} &= f_y u + C\lambda_2 v \\ \frac{\partial v}{\partial \xi} &= f_y v - C\lambda_2 u, \end{aligned} \tag{A9a}$$

with the boundary conditions

$$\begin{aligned} Au(0) + Bu(1) &= 0 \\ Av(0) + Bv(1) &= 0. \end{aligned} \tag{A9b}$$

Because the eigenfunctions are determined up to a multiplicative constant, initial values $u(0)$ and $v(0)$ may be fixed, so the eigenvalue λ_2 and the bifurcation parameter can be found by using a shooting method.

The loci of Hopf and fold bifurcation points meet at a double zero, and the locus of Hopf points has an extreme at a double-Hopf bifurcation. Tracing the locus of Hopf points required the main computing effort. The local parametrization technique (Seydel and Hlavacek, 1987) with secant predictor worked well (only the temperatures $\theta_s(0)$, $\theta_h(0)$, $\theta_t(0)$, and $\theta_r(0)$ were admitted as local parameters). A significant reduction of computing time was achieved by using the Broyden method (instead of Newton) as a corrector. The steplength control strategy recommended by Seydel (1984) was used.

Manuscript received June 22, 1998, and revision received Sept. 28, 1998.